J. Fluid Mech. (1993), *vol.* 252, *pp.* 239–264
Copyright © 1993 Cambridge University Press

Linear acoustic properties of bubbly liquids near the natural frequency of the bubbles using numerical simulations

By A. S. SANGANI AND R. SURESHKUMAR

Department of Chemical Engineering and Materials Science, Syracuse University, Syracuse, NY 13244, USA

(Received 11 August 1992 and in revised form 15 December 1992)

We consider the problem of determining linear acoustic properties of bubbly liquids near the natural frequency of the bubbles. Since the effective wavelength and attenuation length are of the same order of magnitude as the size of the bubbles, we devise a numerical scheme to determine these quantities by solving exactly the multiple scattering problem among many interacting bubbles. It is shown that the phase speed and attenuation are finite at natural frequency even in the absence of damping due to viscous, thermal, nonlinear, and liquid compressibility effects, thus validating a recent theory (Sangani 1991). The results from the numerical scheme are in good agreement with the theory but considerably higher than the experimental values for frequencies greater than the natural frequency. The discrepancy with experiments remains even after accounting for the effect of polydispersity, finite liquid compressibility, and non-adiabatic thermal changes.

1. Introduction

The problem of small-amplitude acoustic wave propagation through bubbly liquids has been examined previously by a number of investigators (Foldy 1945; Carstensen & Foldy 1947; van Wijngaarden 1972; Caflisch *et al.* 1985*a*, *b*; Sangani 1991). When the volume fraction β of gas bubbles is small compared to unity, the speed and attenuation of acoustic waves can be determined to leading order by examining the interaction of a single bubble with the wave. This was done by Foldy (1945) who showed that the effective wavenumber non-dimensionalized by the radius of the bubbles is given by

$$z^2 = z_{\mathrm{L}}^2 + \frac{3\beta\omega_{\mathrm{r}}^2}{1-\omega_{\mathrm{r}}^2(1-\mathrm{i}b)}. \tag{1}$$

The speed of sound C_{ef} in the medium is related to the effective wavenumber by $C_{\mathrm{ef}} = \omega R/z$, where ω is the frequency of the wave and R the radius of the bubbles. In (1), z_{L} is the non-dimensional wavenumber based on the speed of sound in pure liquid, i.e. $z_{\mathrm{L}} = \omega R/C_{\mathrm{L}}$, C_{L} being the speed in pure liquid, and ω_{r} the non-dimensional frequency, i.e. $\omega_{\mathrm{r}} = \omega/\omega_{\mathrm{c}}$, ω_{c} being the natural (resonance) frequency of bubbles approximately given by

$$\omega_{\mathrm{c}}^2 = 3\gamma P_{\mathrm{e}}/\rho_{\mathrm{L}} R^2. \tag{2}$$

Here, γ is the ratio of constant pressure and constant volume specific heats of the gas, ρ_{L} the density of the liquid, and P_{e} the pressure inside the gas bubbles in the absence of wave propagation. Finally, b in (1) is a damping parameter whose magnitude

depends on a number of variables including the viscosity and compressibility of the medium and the thermal properties of the gas (see Commander & Prosperetti 1989, and Sangani 1991, for details). The finite viscosity and non-adiabatic thermal changes are the two principal mechanisms contributing to damping at small frequencies. In addition, damping also occurs due to the finite compressibility of the liquid, which is generally significant at higher frequencies. The pressure disturbance created by the presence of a bubble corresponds to an outgoing scattered wave ($e^{-ik_L r}/r$) in the compressible medium and this consequently gives rise to the damping known as the acoustic radiation damping, which in Foldy's theory is given by (Commander & Prosperetti 1989)

$$b_a = z_L. \tag{3}$$

Here, k_L is the dimensional wavenumber, i.e. $k_L = z_L/R$.

The attenuation predicted by Foldy's theory has been compared with the experimental data reported by several investigators in Commander & Prosperetti (1989). It was found that while the agreement between the theory and experiments was generally good at $\beta < 0.001$, a substantial discrepancy exists for larger β and for frequencies close to and above the natural frequency of the bubbles.

The higher-order corrections to (1) were recently determined by Sangani (1991) who allowed for the interaction among pairs of bubbles. A comparison of this new theory with the experimental data on the attenuation of sound waves reported by Silberman (1957) showed an excellent agreement between the theory and experiments for frequencies smaller than or comparable to the natural frequency of the bubbles, but a poor agreement at higher frequencies. For example, the theory predicted an attenuation of 1.3 dB/cm for bubbles of radii 0.26 cm (natural frequency 1.4 kHz) at 1 kHz frequency and $\beta = 0.01$, which is in perfect agreement with the measured value reported by Silberman (1957). This may be compared with the Foldy theory which predicts an attenuation of only 0.27 dB/cm. On the other hand, the attenuation predicted from the higher-order theory by Sangani is more than twice the experimental value at 7 kHz. This is somewhat surprising since one may expect the interaction effects to become relatively unimportant for frequencies not too close to the resonance frequencies, especially when β is as small as 0.01. It may be added here that the attenuation values predicted by Sangani's theory and thus the higher-order corrections in β actually increase the discrepancy between theory and experiments at higher frequencies. The purpose of the present study therefore is to determine the attenuation of sound waves for random dispersions of gas bubbles in a liquid via direct numerical simulations of the interactions among bubbles to test the theory and to investigate further the reasons for the discrepancy between theory and experiments. Furthermore, as explained in more detail in §2, there were some implicit assumptions made in the higher-order theory by Sangani, and these could be most easily tested through direct numerical simulations.

The organization of this paper is as follows. In §2, we give a brief summary of the important findings of the theory by Sangani and some qualitative differences between that and Foldy's theory. In §3, we present numerical schemes for determining the effective wavenumber in non-dilute bubbly liquids, and, in §4, we compare the results of numerical simulation with various theories and experiments.

2. Background

Sangani (1991) determined the higher-order corrections to (1) when β is small compared to unity but large compared to z_L^2, ω_r being $O(1)$. The ratio of the two terms on the right-hand side of (1) with the damping parameter set to zero is

$$\frac{3\beta\omega_r^2}{z_L^2(1-\omega_r^2)} = \beta\frac{\rho_L C_L^2}{\gamma P_e}\frac{1}{1-\omega_r^2}. \tag{4}$$

For an air–water system at atmospheric pressure, $\rho_L C_L^2/\gamma P_e \sim 10^4$, and, therefore, his theory is expected to apply when $\beta \gg 10^{-4}$ and $\omega_r^2 \ll 10^4\beta$. In this limit, the compressibility of the overall medium is determined primarily by the amount of bubbles and the liquid may be regarded as incompressible. Substituting $z_L = 0$ in (1), we see that the effective wavenumber z is $O(\beta^{\frac{1}{2}})$ in this limit.

Sangani showed that the first correction to (1) is of $O(\beta^{\frac{3}{2}})$:

$$z^2 = z_L^2 + 3\beta t_0[1 - it_0^{\frac{3}{2}}(3\beta)^{\frac{1}{2}}], \quad t_0 = \frac{\omega_r^2}{1-\omega_r^2(1-ib^*)}, \tag{5}$$

where $b^* = b - b_a$ with b_a given by (3). Thus, only the viscous and thermal effects contribute to b^*. Actually, accounting for the thermal effects also changes the natural frequency of the bubbles. The quantities b^* and ω_c are thus to be evaluated from (Prosperetti 1984)

$$b^* = b_v + b_t \equiv \frac{4\mu}{\rho_L R^2\omega} + \frac{P_e\mathscr{H}_I}{\rho_L R^2\omega^2}, \tag{6}$$

$$\omega_c^2 = \frac{3\gamma P_e}{\rho_L R^2}\left[\frac{\mathscr{H}_R}{3\gamma} - \frac{2\sigma}{3R\gamma P_e}\right], \tag{7}$$

where b_v and b_t are, respectively, the viscous and thermal dampings, μ is the viscosity of the liquid, σ is the interfacial tension, and $\mathscr{H}_R$ and $\mathscr{H}_I$ are, respectively, the real and imaginary parts of the complex quantity

$$\mathscr{H} = 3\gamma[1 - 3(\gamma-1)i\alpha^*\{(i/\alpha^*)^{\frac{1}{2}}\coth(i/\alpha^*)^{\frac{1}{2}} - 1\}]^{-1}, \quad \alpha^* = \frac{\alpha_G}{\omega R^2}. \tag{8}$$

Here, α_G is the thermal diffusivity of the gas.

The expression (5) diverges at $\omega_r = 1$ and, hence, it is not suitable for evaluating z in the vicinity of the natural frequency. Sangani therefore rearranged it in the different form given by

$$z^2 = z_L^2 + \frac{3\beta\omega_r^2}{1-\omega_r^2(1-i(b^*+z))}. \tag{9}$$

The two expressions for z, as given by (5) and (9), are the same to $O(\beta^{\frac{3}{2}})$ (provided that $z_L^2 \ll \beta \ll 1$) but the estimates obtained from them for finite β can differ considerably depending on the magnitudes of ω_r and b^*. Comparing now Foldy's expression (1) with the expression (9) obtained by Sangani, we see that the main difference between the two is in the estimate of the acoustic radiation damping: in Foldy's theory $b = b^* + z_L$, and in Sangani's theory $b = b^* + z$. This difference is due to a very simple reason. In the $O(\beta)$ Foldy's theory, the bubbles undergo volume oscillations due to pressure changes in the pure liquid and, thus, it is the compressibility of the liquid that is important, while at small but finite β the overall compressibility of the mixture is governed by the amount of bubbles. Thus, bubbles undergo volume oscillations not in pure liquid but

in a medium that has a much higher compressibility. Sangani also determined the $O(\beta^2 \log \beta)$ and $O(\beta^2)$ corrections to (5), but for now we shall focus on the consequences of the $O(\beta^{\frac{3}{2}})$ theory as given by (9).

Consider first the case $\omega_r < 1$. We shall take β to be comparable to 10^{-2}. If we further take $b^* = 0$ and $z_L = 0$, then z predicted from (1) is real, and the attenuation, which is related to the imaginary part of z, is zero. On the other hand, z computed from (9) is complex and hence there is a finite attenuation even when the damping due to viscous, thermal, and liquid compressibility is taken to be zero. The real part of z is inversely proportional to the phase speed of the wave, and we see that the latter, according to Foldy's theory, approaches zero as $\omega_r \to 1_-$. The phase speed computed from (9), on the other hand, remains finite at $\omega_r = 1$.

The case of $\omega_r \geqslant 1$ is even more interesting. First of all, if we set $b = 0$ in (1), and take z_L to be vanishingly small, then we find that z^2 is a negative number indicating an infinite phase speed and a finite attenuation. This means that most of the sound waves will simply be reflected back from the region of the bubbly liquid, with the intensity of sound waves decreasing exponentially with the distance penetrated by the waves into the bubbly liquid region. This phenomenon can be understood by examining the response of a single bubble to the pressure fluctuations in the medium. It can be shown that the pressure oscillation inside the gas bubble are 180° out of phase with the pressure fluctuations in the liquid when $\omega_r > 1$. Thus, bubbles behave as if their compressibility is negative. Since the compressibility of the liquid is negligible, the overall apparent compressibility of the mixture is negative, and this, in turn, causes the attenuation of sound waves. In most cases, the attenuation due to this overall negative apparent compressibility is far greater in magnitude than that caused by the viscous or thermal effects. The latter effects only cause the phase speed to change from an infinite value to a finite one. For bubbles of 2 mm radius, the magnitude of this phase speed is generally very high, even greater than the speed in pure liquid. At sufficiently large frequencies, the amplitude of the pressure fluctuations in the bubble becomes vanishingly small and hence the apparent negative compressibility of the bubbles becomes nearly zero. Consequently, the liquid compressibility becomes important at high frequencies. This occurs when $z_L^2 \sim 3\beta$ (cf. (1)) or, when $\omega_r \sim 10^2 \beta^{\frac{1}{2}}$ for the air–water system at atmospheric pressure. For even higher frequencies, the bubbles behave essentially like rigid particles and the speed of sound in the medium becomes comparable to that in pure liquid.

The predictions of the $O(\beta^{\frac{3}{2}})$ theory (cf. (9)), on the other hand, are qualitatively different, at least for frequencies close to resonance. In particular, if we take $b^* = z_L = 0$ and $\omega_r = 1$ in (9), then $z^3 = -3i\beta$, and this has three roots given by

$$z = (3\beta)^{\frac{1}{3}} i e^{2i\pi n/3}, \quad n = 0, 1, 2 \quad (\omega_r = 1). \tag{10}$$

Let us define u and v as the real and imaginary parts of the effective wavenumber z, i.e.

$$z = u - iv. \tag{11}$$

The attenuation is then proportional to v, and we shall be interested in the solution of z for which both u and v are non-negative. (The derivation of (9) applied to this case.) This corresponds to $n = 2$ in (10), i.e.

$$z = (3\beta)^{\frac{1}{3}}(\sqrt{3} - i)/2, \tag{12}$$

indicating a finite phase speed and attenuation at $\omega_r = 1$. As ω_r is increased, the magnitude of u decreases up to a value of ω_r roughly given by $\omega_r^{*2} = 1 - 3(3\beta/4)^{\frac{1}{3}})^{-1}$, beyond which z becomes purely imaginary as in Foldy's approximation. Thus,

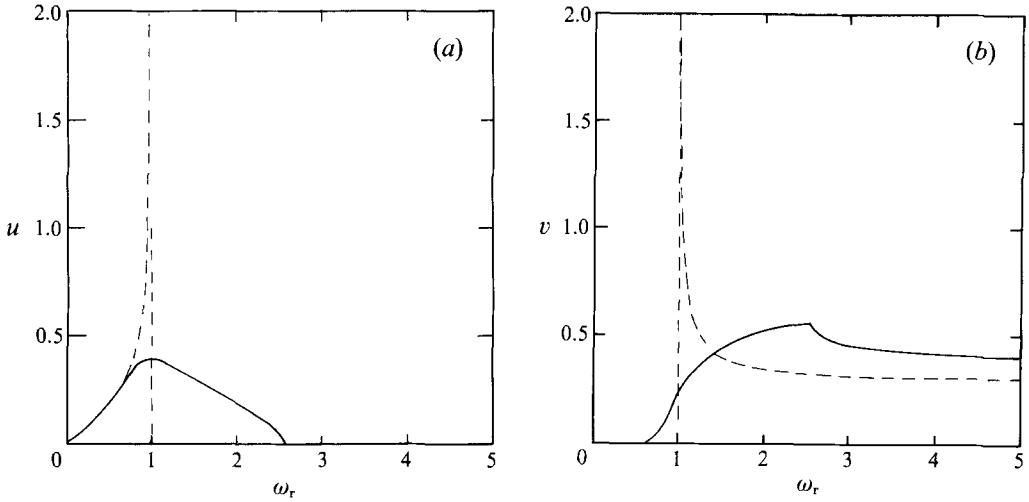

FIGURE 1. A comparison of the real (u) and imaginary (v) parts of the effective wavenumber z predicted by the $O(\beta)$ (dashed line) and $O(\beta^{\frac{3}{2}})$ (solid line) theories. $\beta = 0.03$, $k_L = 0$, and $b^* \approx 0$.

significant differences between the two theories occur in the range $1 < \omega_r < \omega_r^*$ in which the higher-order theory predicts a finite phase speed compared with the infinite speed predicted by Foldy's theory. For $\beta = 0.01$ and 0.03, respectively, ω_r^* equals approximately 1.6 and 2.6, and hence there is a significant range of values of ω_r where the two theories predict different behaviour even for relatively small values of β. These differences for $z_L = b^* = 0$ and $\beta = 0.03$ are shown in figure 1.

The calculation of the $O(\beta^2)$ corrections to Foldy's theory requires the examination of interaction among pairs of bubbles. As shown in more detail in Sangani (1991), a pair of bubbles resonates in two different modes, one in which the two bubbles resonate in phase with each other, and the other in which they are out of phase by 180°. If the non-dimensional interfacial tension is large, the pair of bubbles resonate in the in-phase mode at a frequency that depends on the separation between the two bubbles and varies from $\omega_r = 0.82$ for a pair of nearly touching bubbles, to $\omega_r = 1$ for widely separated bubbles. The out-of-phase mode resonance between pairs of bubbles with large interfacial tension occurs for $\omega_r > 1$. A pair of touching bubbles resonates in this mode at $\omega_r = \infty$ and a pair of widely separated ones at $\omega_r = 1$. Thus, in random dispersions, where the probability density of finding a pair of bubbles with a specified separation distance is finite, there are always pairs of bubbles which are resonating whenever $\omega_r > 0.82$. As shown in Sangani (1991), this causes a logarithmic divergence near $\omega_r = 0.82$ in the $O(\beta^2)$ correction to z^2.

It is important to note that the coefficient of $O(\beta^{\frac{3}{2}})$ in (5) becomes very large in the vicinity of $\omega_r = 1$. Similarly, the coefficients of $O(\beta^2 \log \beta)$ and $O(\beta^2)$ evaluated by Sangani were also large, of $O(10^3)$, for $\omega_r > 0.85$. All these coefficients diverge at $\omega_r = 1$, with the higher-order coefficients diverging more strongly than the lower-order ones. In other words, the asymptotic series for z^2 derived via dilute approximation does not converge for a substantial range of frequencies when β is finite. It may be further noted that, in dispersions containing many bubbles, the resonances between groups of three or more bubbles can also become significant, and since these resonances occur for an even larger range of frequencies, it is unclear how accurate the predictions of the dilute theories, which only examine the interaction of a single or a pair of bubbles with the wave, will be when β is finite. On the other hand, if the predictions of the modified

$O(\beta^{\frac{3}{2}})$ theory (cf. (9)), according to which the acoustic response of bubbly liquids is finite even at the primary resonance frequency ($\omega_r = 1$), are indeed correct, then one would expect the resonance effects of two or more bubbles to play a relatively unimportant role in determining the acoustic properties of the bubbly liquids. Since the modified theory (9) is only one of many other ways in which the divergent series (5) can be recast, it is important to test it by carrying out direct numerical simulations of the multiple scattering problem. Indeed, implicit in rearranging the original asymptotic series into (9) is an assumption that z will be finite at $\omega_r = 1$ even when the thermal, viscous, liquid compressibility, and nonlinear effects are neglected.

Since the wavenumber is $O(1)$ when β is $O(1)$, or when the resonance effects become important, we devise in this paper a novel scheme for determining the interaction among bubbles in which the smallness of z is not assumed, as is typically the case with most dilute theories. The results of numerical simulations verify the predictions of $O(\beta^{\frac{3}{2}})$ theory (cf. (12)) at $\omega_r = 1$ and small β. The departure of numerical simulation results from the theory, however, becomes significant at $\beta = 0.01$, where the exact results deviate from theory by a factor of 2. Thus, the higher-order interactions are significant even for β as small as 0.01. The agreement between theory and simulations is much better for larger frequencies, and we find that both the theory and simulations results for attenuations are higher than those predicted from Foldy's theory, which, in turn, are higher than the experimental values reported by Silberman (1957). We have investigated the effects of finite compressibility of the liquid and polydispersity, in addition to the multi-bubble interactions via numerical simulations, but none of these factors reduces the gap between theory and experiments.

3. Formulation of the problem and the method of solution

As discussed in the previous sections, there are two main objectives of the present study. The first is to test the validity of the dilute theories due to Foldy and Sangani, and for this purpose we shall restrict our attention to the case $b^* = 0$ for which the differences in the prediction of the two theories are most significant, particularly near $\omega_r = 1$. The case $b^* = 0$ corresponds to no thermal or viscous damping. The second objective is to examine the reason for the discrepancy between the theory predictions and the experimental data on attenuation of sound waves by Silberman (1957) which were carried out for bubbles with approximate radius of 0.26 cm and for $\beta = 0.01$. As noted in Sangani (1991), the thermal damping is significant for this size of bubbles, and therefore we should account for the thermal effects in comparing the results of numerical simulations with the experiments. The viscous effects are negligible for these experimental conditions. Finally, the finite compressibility of the liquid may also become important at large frequencies, and therefore our numerical simulations should allow for it also. This will be particularly important at the larger frequencies where the thermal and viscous effects generally become unimportant and where a substantial discrepancy between theory and experiments exists. It may be noted that the theory of Sangani ignored liquid compressibility, thus the addition of z_L^2 in (9) is somewhat arbitrary. This was added simply to have the correct leading-order behaviour for z for $\beta \to 0$ or $\omega_r \to \infty$. Thus, we shall formulate the problem accounting for both thermal and compressibility effects but ignore viscous effects. The special case $b^* = 0$ can then be recovered from our solution by taking the appropriate limit. There is also a slight advantage in keeping the compressibility of the liquid in the formulation as the long-range interactions are then easy to sum. The case of negligible compressibility can be deduced by taking the limit $k_L \to 0$ once these interactions are properly summed.

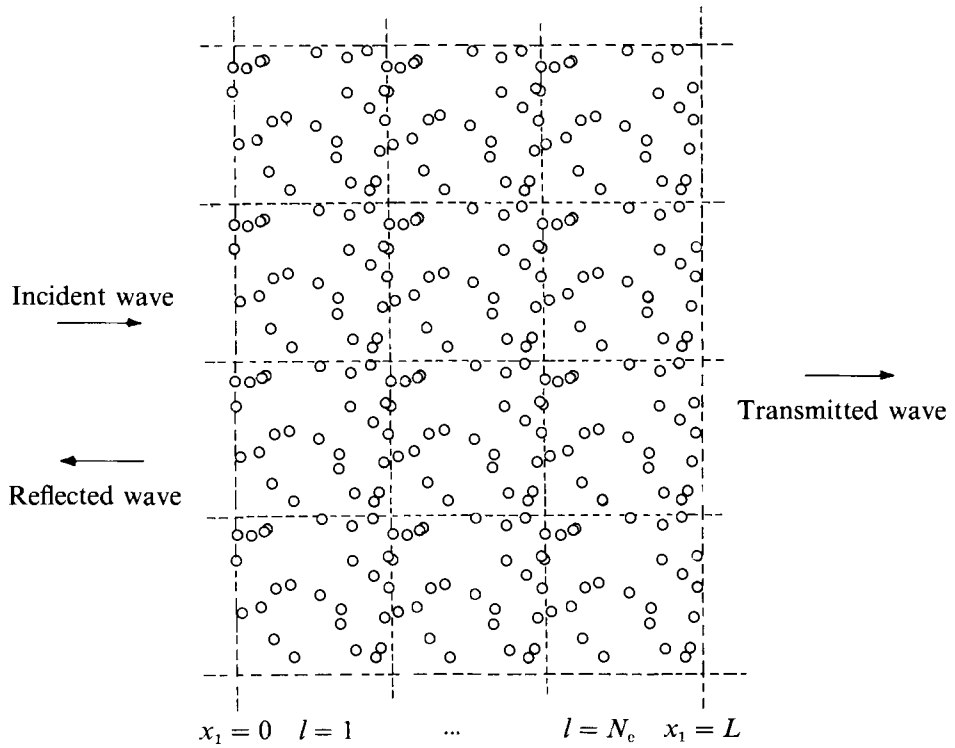

FIGURE 2. A schematic of the problem. The finite bubbly region in $0 \leqslant x_1 \leqslant L$ is assumed to consist of identical cubes each containing N randomly placed bubbles.

In theories for small β, the effective wavenumber z is taken to be small, of $O(\beta^{\frac{1}{2}})$. As mentioned in §2, the magnitude of the wavenumber, however, can be comparable to unity close to resonance frequencies even for β as small as 0.01. Therefore, we treat z as $O(1)$. To determine z, we formulate the problem in the following manner. First, we assume that we have a region of bubbly liquid of finite thickness L in the x_1-direction and of infinite width in the x_2- and x_3-directions (cf. figure 2). This region is surrounded on both sides by pure liquid. Next, we assume that a planar acoustic wave is incident upon this bubbly region. The average pressure or velocity amplitude will, of course, vary with x_1 in the bubbly region, but if L is much larger than the effective wavelength of the wave in the bubbly region, then we expect the effective wavenumber in the bulk of the bubbly region, i.e. away from $x_1 = 0$, L, to become independent of the nature of boundary conditions imposed at $x_1 = \pm\infty$. It is this behaviour in the bulk that we shall be mostly interested in examining.

A commonly used procedure for formulating such problems is the method of homogenization (Keller 1977; Bensoussan, Lions & Papanicolaou 1978; Sanchez-Palencia 1980) which treats various dynamic variables as functions of two spatial variables, one accounting for the slow variations due to the passage of the wave and the other accounting for the rapid variations caused by the presence of bubbles. Using this method, it is then possible to define the problem to be solved for the rapid variations. Such a procedure was employed by Caflisch *et al.* (1985*a*, *b*), Rubinstein (1985), and Miksis & Ting (1987*a*, *b*) for determining z for dilute bubbly liquids. Since the effective wavelength is $O(1)$ when β is $O(1)$, there is no clear distinction of lengthscales in the present case and, therefore, this method is not suitable for our purpose.

We divide the bubbly region into cubes of size h, each containing a total of N randomly placed bubbles. The centres of these bubbles are given by

$$\boldsymbol{x}^{\alpha L} = \boldsymbol{y}^{\alpha} + \boldsymbol{x}_{\mathrm{L}}, \quad \boldsymbol{x}_{\mathrm{L}} = h[(l-1)\,\boldsymbol{e}_1 + m\boldsymbol{e}_2 + n\boldsymbol{e}_3], \tag{13}$$

with $\alpha = 1, 2, \ldots, N, l = 1, 2, \ldots N_{\mathrm{c}}$, and $m, n = 0, \pm 1, \pm 2, \ldots \pm \infty$. Here, $\boldsymbol{e}_1, \boldsymbol{e}_2$, and $\boldsymbol{e}_3$ are the unit vectors along the three coordinate axes, and $N_{\mathrm{c}} = L/h$. Since the viscous effects are neglected, the equations of motion for small-amplitude waves reduce to

$$\nabla^2 p + k_{\mathrm{L}}^2 p = 0, \tag{14}$$

where p is the amplitude of the pressure disturbance at a point $\boldsymbol{x}$ in the liquid, and k_{L} the dimensional wavenumber in pure liquid, i.e. $k_{\mathrm{L}} = z_{\mathrm{L}}/R = \omega/C_{\mathrm{L}}$. All disturbance quantities will be assumed to depend on time as $\mathrm{e}^{\mathrm{i}\omega t}$. The boundary conditions for p on the surface of each bubble are derived in Sangani (1991). He expanded p near the surface of each bubble in terms of Legendre polynomials as

$$p = \sum_{n=0}^{\infty} \sum_{m=0}^{n} [p_{nm}(r) \cos m\phi + \tilde{p}_{nm}(r) \sin m\phi]\, P_n^m(\cos\theta), \tag{15}$$

where r, θ, and ϕ are measured with respect to the centre of the bubble. If the viscous and thermal effects are neglected, the kinematic and dynamic stress conditions at the surface of the bubbles can be combined to give (Sangani 1991)

$$p_{nm}(R) = \sigma^*[2 - n(n+1)]\, R p'_{nm}(R) \quad \text{for} \quad n > 0, \quad \omega_{\mathrm{r}}^2 p_{00}(R) + R p'_{00}(R) = 0, \tag{16}$$

where R is the radius of the bubble, $\sigma^* = \sigma/\rho_{\mathrm{L}} R^3 \omega^2$ the non-dimensional interfacial tension, and the prime denotes the differentiation with respect to r. The same conditions also apply to $\tilde{p}_{nm}(r)$, with $\tilde{p}_{n0}(r) \equiv 0$. The modification to (16) to account for the non-adiabatic thermal effects will be discussed later.

In addition to the above conditions at the surface of the bubbles, we also need to specify the conditions at $x_1 = \pm\infty$. We shall assume that a planar wave of unit magnitude is incident upon the bubbly region. Far away from the bubbly region, there will also be planar waves scattered from the region. Thus we have the conditions

$$p \to \mathrm{e}^{-\mathrm{i}k_{\mathrm{L}}x_1} + F_{\mathrm{r}}\, \mathrm{e}^{\mathrm{i}k_{\mathrm{L}}x_1} \quad \text{as} \quad x_1 \to -\infty \tag{17}$$

and

$$p \to F_{\mathrm{t}}\, \mathrm{e}^{-\mathrm{i}k_{\mathrm{L}}x_1} \quad \text{as} \quad x_1 \to \infty, \tag{18}$$

where F_{r} and F_{t} are the amplitudes of the reflected and transmitted waves whose values are to be determined as a part of the solution. This completes the formulation of the problem. The determination of the effective wavenumber from the solution of this problem will be discussed later.

To obtain the solution of the above problem, we exploit the periodicity of p in the plane perpendicular to the direction of wave propagation. Let G denote the fundamental singular solution (Green's function) of the Helmholtz equation which is periodic in planes perpendicular to the x_1-axis, i.e. let

$$(\nabla^2 + k_{\mathrm{L}}^2)\, G(\boldsymbol{x}) = -4\pi \sum_{\boldsymbol{R}_{\mathrm{L}}} \delta(\boldsymbol{x} - \boldsymbol{R}_{\mathrm{L}}), \quad \boldsymbol{R}_{\mathrm{L}} = h(m\boldsymbol{e}_2 + n\boldsymbol{e}_3), \tag{19}$$

with $m, n = 0, \pm 1, \pm 2, \ldots$. To obtain unique solutions to the Helmholtz equation, we must also specify the correct radiation condition. In the present case, this corresponds to an outgoing planar wave away from the scatterers. Thus, we require that

$$G(\boldsymbol{x}) \to c\, \mathrm{e}^{-\mathrm{i}k_{\mathrm{L}}|x_1|} \quad \text{as} \quad |x_1| \to \infty, \tag{20}$$

where c is a constant to be determined. We therefore write

$$G(\boldsymbol{x}) = c\,\mathrm{e}^{-\mathrm{i}k_{\mathrm{L}}|x_1|} + H(\boldsymbol{x}), \tag{21}$$

with $H \to 0$ as $|x_1| \to \infty$, and

$$(\nabla^2 + k_{\mathrm{L}}^2)\,H(\boldsymbol{x}) = -4\pi \sum_{\boldsymbol{R}_{\mathrm{L}}} \delta(\boldsymbol{x} - \boldsymbol{R}_{\mathrm{L}}) + 2\mathrm{i}k_{\mathrm{L}}\, c\delta(|x_1|). \tag{22}$$

We further impose the condition that the average of H on any plane perpendicular to the x_1-axis be zero. This requires that the integration of the right-hand side of (22) on the plane $x_1 = 0$ be zero or

$$c = 2\pi/\mathrm{i}k_{\mathrm{L}}h^2. \tag{23}$$

The expressions for evaluating H are given in Appendix A, where it is shown that H decays exponentially with $|x_1|$ within a distance comparable to h (cf. (A 2)). Thus, H represents the short-range effect of the point scatterers on the lattice. The other part of G, i.e. $c\,\mathrm{e}^{-\mathrm{i}k_{\mathrm{L}}|x_1|}$, represents the long-range effect since k_{L} is usually small and real.

Now an expression for p can be obtained by the method of multipole expansions. The basic idea is that since the derivatives of G are also solutions of the Helmholtz equation, and since the governing equations are linear, a general solution for p is a linear combination of these derivatives. In the present case, we have a total of $N \times N_{\mathrm{c}}$ doubly periodic lattices of bubbles and the response of each of them can be superimposed. Thus, we write

$$p(\boldsymbol{x}) = \mathrm{e}^{-\mathrm{i}k_{\mathrm{L}}x_1} + \sum [A_{nm}^{\alpha l}\,\mathscr{D}_{nm} + \tilde{A}_{nm}^{\alpha l}\,\tilde{\mathscr{D}}_{nm}]\,G(\boldsymbol{x} - \boldsymbol{x}_1^{\alpha l}), \tag{24}$$

where the summation is over α (1 to N), l (1 to N_{c}), n (0 to ∞), and m (0 to n), and $\boldsymbol{x}_1^{\alpha l} = x_1^{\alpha l}\boldsymbol{e}_1 = (y_1^{\alpha} + (l-1)\,h)\,\boldsymbol{e}_1$. $A_{nm}^{\alpha l}$ and $\tilde{A}_{nm}^{\alpha l}$ are the unknown coefficients to be determined from the boundary conditions, and are referred to as the strengths of the 2^n-multipoles. $\mathscr{D}_{nm}$ and $\tilde{\mathscr{D}}_{nm}$ are the differential operators related to the solid spherical harmonics Y_n^m and $\tilde{Y}_n^m$ by

$$\mathscr{D}_{nm} = Y_n^m\left(\frac{\partial}{\partial x_1}, \frac{\partial}{\partial x_2}, \frac{\partial}{\partial x_3}\right), \quad \tilde{\mathscr{D}}_{nm} = \tilde{Y}_n^m\left(\frac{\partial}{\partial x_1}, \frac{\partial}{\partial x_2}, \frac{\partial}{\partial x_3}\right), \tag{25}$$

where Y_n^m and $\tilde{Y}_n^m$ are given by

$$Y_n^m(x_1, x_2, x_3) = r^n\,P_n^m(\cos\theta)\cos m\phi, \quad \tilde{Y}_n^m(x_1, x_2, x_3) = r^n\,P_n^m(\cos\theta)\sin m\phi, \tag{26}$$

with $x_1 = r\cos\theta$, $x_2 = r\sin\theta\cos\phi$, and $x_3 = r\sin\theta\sin\phi$.

It may be noted that the transmitted and reflected wave coefficients (cf. (17) and (18)), if required, can be evaluated from the strengths of multipoles by means of

$$F_{\mathrm{t}} = c\sum A_{n0}^{\alpha l}(-\mathrm{i}k_{\mathrm{L}})^n\,\mathrm{e}^{\mathrm{i}k_{\mathrm{L}}x_1^{\alpha l}}, \quad F_{\mathrm{r}} = c\sum A_{n0}^{\alpha l}(\mathrm{i}k_{\mathrm{L}})^n\,\mathrm{e}^{-\mathrm{i}k_{\mathrm{L}}x_1^{\alpha l}}, \tag{27}$$

where we have made use of the behaviour of G at $x_1 = \pm\infty$ (cf. (20)) and of the relations

$$\mathscr{D}_{nm}\,\mathrm{e}^{\mathrm{i}k_{\mathrm{L}}x_1} = (\mathrm{i}k_{\mathrm{L}})^n\,\delta_{m0}\,\mathrm{e}^{\mathrm{i}k_{\mathrm{L}}x_1}, \quad \tilde{\mathscr{D}}_{nm}\,\mathrm{e}^{\mathrm{i}k_{\mathrm{L}}x_1} = 0. \tag{28}$$

The expression (24) for p is valid at all points in the liquid. To determine the unknowns $A_{nm}^{\alpha l}$, it is convenient to express p near the surface of each bubble as given by (15) with $p_{nm}(r)$ written as a sum of singular and regular (at $r = 0$) spherical Bessel functions of degree n. There are three different singular spherical Bessel functions for each n, and we must choose the one that corresponds to the singular behaviour of G near $r = 0$. As shown in Appendix A, this behaviour corresponds to a standing wave, i.e. $G \to \cos k_{\mathrm{L}}r/r = -k_{\mathrm{L}}y_0(k_{\mathrm{L}}r)$. We therefore choose $p_{nm}(r)$ to be given by

$$p_{nm}(r) = C_{nm}j_n(k_{\mathrm{L}}r) + E_{nm}\,y_n(k_{\mathrm{L}}r), \tag{29}$$

where j_n and y_n are the spherical Bessel functions of first and second kinds, respectively (Abramowitz & Stegun 1972). It may be noted that this expression for p_{nm} is different from the one employed by Sangani (1991) who used the spherical Bessel functions of the third kind (h_n) instead of the second kind (y_n). In that problem, the conditionally averaged pressure field consisted of a sum of a mean planar wave and an outgoing spherical wave from the surface of the bubble. In numerical simulations, we need to impose periodicity, and this forces the singular behaviour near the lattice points to be that corresponding to a standing wave. Of course, far from any plane of bubbles, G still has a behaviour corresponding to an outgoing planar wave and thus the radiation condition at infinity is satisfied. Actually, as explained in Appendix A, the imposed periodicity in the plane transverse to the wave propagation does pose some problems in modelling the behaviour of truly random dispersions. This is so because the solution of (19) in the limit $k_{\mathrm{L}}h \to \infty$ is not well behaved owing to the resonance effects of the period lattices. Since $h \to \infty$ as $N \to \infty$ for a given β, the influence of the imposed periodicity would be particularly severe for a sufficiently large N. The simulations in the present study are carried out, however, only for $N \leqslant 200$, and $k_{\mathrm{L}}h$ for these simulations is small enough not to cause the resonance of the lattice. Moreover, a major portion of the results presented here is concerned with assessing the dilute theory which was carried out for $k_{\mathrm{L}} = 0$, and for this purpose it is appropriate to take the limit $k_{\mathrm{L}}h \to 0$ before taking the limit $N \to \infty$.

The constants C_{nm} and E_{nm} in (29) are different for each bubble and superscripts will be used to denote the particular bubbles to which they refer. The singular terms in (29) for the bubble αl can arise only from the terms in (24) that are singular at $\boldsymbol{x}^{\alpha l}$. Now, employing a differentiation theorem from the monograph by Hobson (1931, p. 127), it can be shown that

$$\mathscr{D}_{nm}\, y_0(k_{\mathrm{L}} r) = (-k_{\mathrm{L}})^n\, y_n(k_{\mathrm{L}} r)\, P_n^m(\cos\theta)\cos m\varphi. \tag{30}$$

Combining (24), (29), and (3), we therefore obtain

$$E_{nm}^{\alpha l} = (-k_{\mathrm{L}})^{n+1}\, A_{nm}^{\alpha l}. \tag{31}$$

A similar relation applied for $\tilde{E}_{nm}^{\alpha l}$ and $\tilde{A}_{nm}^{\alpha l}$. The terms in (24) that are regular at $\boldsymbol{x}^{\alpha l}$ must be related to the regular terms in (29). Let $p_{\mathrm{r}}^{\alpha l}$ denote the regular part, i.e. let

$$p_{\mathrm{r}}^{\alpha l} = \mathrm{e}^{-\mathrm{i}k_{\mathrm{L}}x_1} + \sum [A_{rs}^{\gamma j}\, \mathscr{D}_{rs} + \tilde{A}_{rs}^{\gamma j}\, \tilde{\mathscr{D}}_{rs}]\, G^*(\boldsymbol{x} - \boldsymbol{x}^{\gamma j}), \tag{32}$$

where the summation is to be carried out for all γ, j, r, and s, and G^* is defined as $G^*(\boldsymbol{x}-\boldsymbol{x}^{\gamma j}) = G(\boldsymbol{x}-\boldsymbol{x}^{\gamma j}) - \cos(k_{\mathrm{L}} r)/r$ with $r = |\boldsymbol{x}-\boldsymbol{x}^{\gamma j}|$ for $(\gamma, j) = (\alpha, l)$, and $G^* = G$ otherwise. In other words, G and G^* are the same except for the bubble αl, for which the difference between the two corresponds to the singular part. Thus, we have

$$p_{\mathrm{r}}^{\alpha l} = \sum_{n=0}^{\infty} \sum_{m=0}^{n} (C_{nm}^{\alpha l} \cos m\varphi + \tilde{C}_{nm}^{\alpha l} \sin m\varphi)\, j_n(k_{\mathrm{L}} r)\, P_n^m(\cos\theta). \tag{33}$$

Now multiplying both sides of (33) with $P_n^m(\cos\theta)\cos m\varphi$, integrating over the surface of the bubble, and using an integration theorem of Hobson (1931, p. 161), we obtain

$$C_{nm}^{\alpha l} = \frac{2(2n+1)\,(n-m)!}{\epsilon_m (n+m)!} k_{\mathrm{L}}^{-n}\, \mathscr{D}_{nm}\, p_{\mathrm{r}}^{\alpha l}(\boldsymbol{x}^{\alpha l}), \tag{34}$$

where $\epsilon_m = 1$ for $m > 0$ and $\epsilon_0 = 2$. Finally, a relation between $C_{nm}^{\alpha l}$ and $E_{nm}^{\alpha l}$ can be obtained by substituting (29) into (16), and combining it with (31) and (34), we obtain

$$t_{nm}\, A_{nm}^{\alpha l} = \mathscr{D}_{nm}\, p_{\mathrm{r}}^{\alpha l}(\boldsymbol{x}^{\alpha l}), \tag{35}$$

where t_{nm} is given by

$$t_{nm} = \epsilon_m(-1)^{n+1}\frac{k_L^{2n+1}(n+m)!}{2(2n+1)(n-m)!}\frac{z\sigma^*(2-n(n+1))\,y_n'-y_n}{j_n-z\sigma^*(2-n(n+1))j_n'}, \quad n \geqslant 1, \tag{36}$$

$$t_{00} = k_L\frac{y_0\omega_r^2+zy_0'}{j_0\omega_r^2+zj_0'}. \tag{37}$$

Here, the functions j_n and y_n, and their derivatives j_n' and y_n', are to be evaluated at $z_L = k_L R$. When the bubbly liquid is not monodisperse, we should replace R in the above expression by the radius of the bubble αl. Since the compressibility of the liquid is small, we can use the limiting form of the above expression by substituting $y_n = -(2n-1)!!\,z_L^{-n-1}, j_n = z^n/(2n+1)!!$ for $n \geqslant 1$ and $y_0 = -z^{-1}, j_0 = 1$. In particular, the equation for t_{00} simplifies to

$$t_{00} = \frac{1-\omega_r^2}{R\omega_r^2} \tag{38}$$

with the relative error of $O(z_L^2)$. The expression for $\tilde{A}_{nm}^{\alpha l}$ can be obtained by replacing $\mathscr{D}_{nm}$ in (35) by $\tilde{\mathscr{D}}_{nm}$.

The above expressions are valid provided that viscous and thermal effects are negligible. As shown in Sangani (1991), the thermal effects only affect the expression for t_{00} because they force variations in only the spherically symmetric part (p_{00}) of the pressure. Thus, to account for the thermal effects, we need to modify the expression for t_{00} to

$$t_{00} = \frac{1-\omega_r^2(1-ib_t)}{R\omega_r^2}, \tag{39}$$

where b_t is the thermal damping as given by the second term on the right-hand side of (6). Note that in evaluating $\omega_r = \omega/\omega_c$, we must use (7) to calculate ω_c whenever the thermal effects are included in the calculations. Allowing for the viscous effects will modify the expressions for all t_{nm} but, as mentioned earlier, we shall neglect viscous effects in the present study. These effects are most significant at low frequencies, and a recent study by Sangani, Zhang & Prosperetti (1991) has examined them in detail.

Now, as noted earlier, the first term on the right-hand side of (21) represents the behaviour of G at large distances from the plane of singularities. It is convenient to separate this long-range contribution from the short-range one in the solving for $A_{nm}^{\alpha l}$. Thus, we rewrite (35) as

$$t_{nm}A_{nm}^{\alpha l} = \delta_{m0}P_n^{\alpha l} + \sum_{r,s,\gamma,j}[A_{rs}^{\gamma j}\mathscr{D}_{rs} + \tilde{A}_{rs}^{\gamma j}\tilde{\mathscr{D}}_{rs}]\mathscr{D}_{nm}H^*(\boldsymbol{x}^{\alpha l}-\boldsymbol{x}^{\gamma j}), \tag{40}$$

where H^* is the regular part of H at $\boldsymbol{x}^{\alpha l}$. Since the singularities of $H(\boldsymbol{x})$ lie on the plane $x_1 = 0$, the singular part of H equals $\cos k_L r/r + ic \sin k_L|x_1|$ (cf. Appendix A) and H^* is obtained by subtracting this singular part from H for $(\alpha, l) = (\gamma, j)$. H^* decreases exponentially with distance from the plane of singularities, and the summation term in (40) therefore represents the short-range interaction effects. The long-range interaction part $P_n^{\alpha l}$ is given by

$$P_n^{\alpha l} = \left[\frac{\partial^n}{\partial x_1^n}e^{-ik_L x_1} + c\sum_{r,\gamma,j}A_{r0}^{\gamma j}\frac{\partial^{r+n}}{\partial x_1^{r+n}}\{e^{-ik_L|x_1-x_1^{\gamma j}|} + i\sin(k_L|x_1-x_1^{\gamma j}|)\,\delta_{\alpha\gamma}\delta_{ij}\}\right]_{x_1=x_1^{\alpha l}}. \tag{41}$$

The equation for $\tilde{A}^{\alpha j}_{nm}$ contains only the short-range interactions:

$$t_{nm}\tilde{A}^{\alpha l}_{nm} = \sum_{r,s,\gamma j} [A^{\gamma j}_{rs}\mathscr{D}_{rs} + \tilde{A}^{\gamma j}_{rs}\tilde{\mathscr{D}}_{rs}]\tilde{\mathscr{D}}_{nm} H^*(\boldsymbol{x}^{\alpha l} - \boldsymbol{x}^{\gamma j}). \tag{42}$$

The set of linear equations given by (40) and (42) provides a sufficient number of relations for determining all the unknowns $A^{\alpha l}_{nm}$ and $\tilde{A}^{\alpha l}_{nm}$. This set can be truncated to $n \leqslant N_s$ resulting in a total of $(N_s+1)^2 N N_c$ linear equations in an equal number of unknowns. Our main aim is to determine the effective wavenumber for the bulk of the bubbly liquid, i.e. for the region in which the end effects due to the finite width of the bubbly region are not important. For this purpose, we seek the solution of these equations in the bulk ($1 \ll l \ll N_c$) in the form

$$A^{\alpha l}_{nm} = B^{\alpha}_{nm}\, e^{i\Gamma x_1^{\alpha l}} + B'^{\alpha}_{nm}\, e^{i\Gamma' x_1^{\alpha l}}, \tag{43}$$

with a similar relation for $\tilde{A}^{\alpha l}_{nm}$. According to these expressions, the multipoles of the bubbles in one cell are related to those in the other by a simple wave modulation. This particular form for the solution in the bulk has been used previously by Twersky (1962). Γ and Γ' are the dimensional effective wavenumbers corresponding to the waves travelling along the positive and negative x_1-axes, and $i\Gamma$ and $i\Gamma'$ are complex conjugates. The non-dimensional effective wavenumber is given by $z = u - iv = -\Gamma R$.

Substitution of (43) into (40)–(42) produces terms that are proportional to any one of the four terms $e^{-ik_L x_1^{\alpha l}}$, $e^{ik_L x_1^{\alpha l}}$, $e^{i\Gamma x_1^{\alpha l}}$, and $e^{i\Gamma' x_1^{\alpha l}}$, of which the terms of the first two kinds are unimportant if our goal is only to determine the effective wavenumber in the bulk. Comparing the coefficients of the terms proportional to $e^{i\Gamma x_1^{\alpha l}}$ yields the following set of equations (see Appendix B for details):

$$t_{nm}B^{\alpha}_{nm} = F^{\alpha}_n \delta_{m0} + \sum_{r,s,\gamma} [B^{\gamma}_{rs}\mathscr{D}_{rs} + \tilde{B}^{\gamma}_{rs}\tilde{\mathscr{D}}_{rs}]\mathscr{D}_{nm}\, e^{i\Gamma(y_1^{\gamma} - y_1^{\alpha})} S^*(\boldsymbol{y}^{\alpha} - \boldsymbol{y}^{\gamma}), \tag{44}$$

with

$$F^{\alpha}_n = (-ik_L)^n F^{\alpha}_- + (ik_L)^n F^{\alpha}_+, \tag{45}$$

$$F^{\alpha}_{\mp} = \pm c \sum_{r,\gamma} B^{\gamma}_{r0}(\mp ik_L)^r e^{i(\Gamma \pm k_L)(y_1^{\alpha} - y_1^{\gamma})} \left[\frac{1}{e^{ih(\Gamma \pm k_L)} - 1} + \lambda_{\alpha\gamma}\right], \tag{46}$$

$$\lambda_{\alpha\gamma} = g(y_1^{\alpha} - y_1^{\gamma}), \tag{47}$$

where $g(y)$ is the Heavyside step function whose value is unity for $y > 0$, zero for $y < 0$, and one-half for $y = 0$. Similarly, we have

$$t_{nm}\tilde{B}^{\alpha}_{nm} = \sum_{r,s,\gamma} [B^{\gamma}_{rs}\mathscr{D}_{rs} + \tilde{B}^{\gamma}_{rs}\tilde{\mathscr{D}}_{rs}]\tilde{\mathscr{D}}_{nm}\, e^{i\Gamma(y_1^{\gamma} - y_1^{\alpha})} S^*(\boldsymbol{y}^{\alpha} - \boldsymbol{y}^{\gamma}). \tag{48}$$

The function S^* is related to H^* by

$$S^*(\boldsymbol{x}) = \sum_{l=-\infty}^{\infty} H^*(\boldsymbol{x} + lh\boldsymbol{e}_1)\, e^{-i\Gamma l h}. \tag{49}$$

Now (44) and (48) together constitute a homogeneous set of infinite linear equations in B^{α}_{nm} and $\tilde{B}^{\alpha}_{nm}$. The solvability condition for a non-trivial solution to this set gives a necessary condition for determining the effective wavenumber Γ. After truncating this set to $n \leqslant N_s$, the resulting equations can be recast into a vector relation

$$U_{ij} X_j = 0,\ i = 1, 2, \ldots, N(N_s+1)^2,$$

in which X_j is the vector of (complex) unknowns, B^{α}_{nm} and $\tilde{B}^{\alpha}_{nm}$. The solvability condition is that the determinant of U_{ij} must vanish. This condition, however, is

difficult to implement numerically since the size of the matrix U_{ij} is typically very large, and, consequently, the determinant is difficult to evaluate.

We use two different methods for determining Γ. The first is an iterative method in which we fix one of the unknowns, say B^1_{00}, to unity and remove the corresponding equation, i.e. the one corresponding to $n = m = 0$ and $\alpha = 1$, from the above set of equations. The remaining inhomogeneous set of equations can now be solved for an assumed value of Γ. Once all the unknowns are determined, their values can be substituted into the equation that was removed to check if the assumed value of Γ is correct. Otherwise, a different guess is chosen for Γ until all the equations are satisfied. This is a somewhat cumbersome two-dimensional search since Γ is complex, but manageable since we do not need to obtain results over a wide range of β and ω_r.

The second method, to be referred to as the direct method, consists of solving the full inhomogeneous set of equations as give by (40) and (42). Since this method is not iterative, it can be used for larger values of N. Once all the multipoles $A^{\alpha l}_{nm}$ and $\tilde{A}^{\alpha l}_{nm}$ are determined, Γ can be determined by a least-squares method by best fitting the multipoles' values to expressions such as (43) applicable for bubbles located in the bulk of the bubbly region. Here, by bulk we mean the region that is obtained by removing 10% of the bubbly liquid from either side of the bubbly region, i.e. $0.1\,L < x_1 < 0.9\,L$ (cf. figure 2). In these calculations N_c was chosen to be unity. This method was used only for determining attenuation at higher frequencies ($\omega_r > \omega_r^*$) for which the real part of Γ is negligibly small and $\Gamma \approx \Gamma'$. Thus, the least-square fitting is done only for one variable, namely the imaginary part of Γ.

For testing the validity of the $O(\beta^{\frac{3}{2}})$ theory by Sangani (1991), we can set the liquid compressibility to zero as mentioned earlier. It can be shown that F^α_n in (45) can be evaluated in the limit $k_L \to 0$ from

$$F^\alpha_1 = -\frac{4\pi}{h^2}\sum_{\gamma=1}^{N}\left(\frac{1}{e^{i\Gamma h}-1}+\lambda_{\alpha\gamma}\right)B^\gamma_{00}\,e^{i\Gamma(y_1^\gamma-y_1^\alpha)}, \quad F^\alpha_n = 0, \quad n > 1, \tag{50}$$

$$F^\alpha_0 = \frac{4\pi}{h^2}\sum_{\gamma=1}^{N}\left[\left\{(y_1^\gamma-y_1^\alpha)\left(\frac{1}{e^{i\Gamma h}-1}+\lambda_{\alpha\gamma}\right)-\frac{h\,e^{i\Gamma h}}{(e^{i\Gamma h}-1)^2}\right\}B^\gamma_{00} - \left(\frac{1}{e^{i\Gamma h}-1}+\lambda_{\alpha\gamma}\right)B^\gamma_{10}\right]e^{i\Gamma(y_1^\gamma-y_1^\alpha)}. \tag{51}$$

As shown in Appendix C, the special cases of dilute random and periodic arrays treated, respectively, by Foldy (1945) and Rubinstein (1985) can be derived from the general equations presented in this section.

4. Results

The method described in the previous section can be used for determining the attenuation and phase speed for arbitrary volume fractions. However, since our primary interest is in testing the validity of dilute theories, we shall present results only for relatively low volume fractions. Also, the attenuation of sound waves near natural frequencies for volume fractions greater than a few percent is so high that it becomes somewhat meaningless to determine it for the bulk of the bubbly region.

4.1. *Comparison with theory*

As mentioned in the Introduction, we test the validity of the theory for the simplest case in which the compressibility of the liquid and the viscous and thermal effects are neglected. In this subsection, therefore, we present results obtained with $k_L = b^* = 0$.

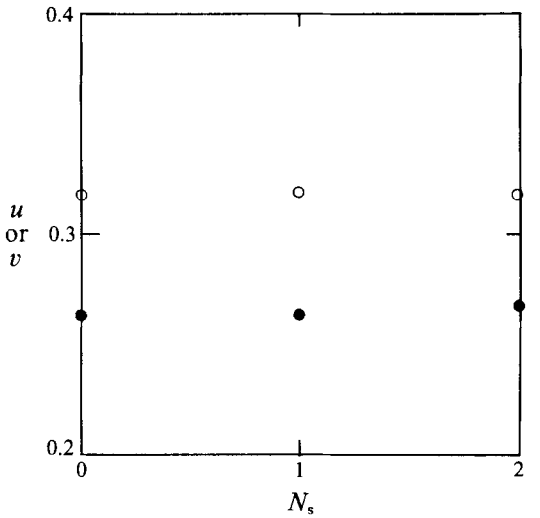

FIGURE 3. The real (open circles) and imaginary (filled circles) parts of z as a function of N_s, the highest order of singularities retained in solving the scattering problem. $\beta = 0.01$, $\omega_r = 1$, and $N = 16$.

The computer program for determining z by the iterative method was first tested for the special case of periodic arrays with small β for which the analysis of Rubinstein (1985) should apply. This corresponds to $N = 1$. His result with $k_L = 0$ reads

$$z^2 = -3\beta\Omega(1 + 1.7601\beta^{\frac{1}{3}}\Omega + O(\beta^{\frac{2}{3}})), \tag{52}$$

where $\Omega = \omega_r^2/(\omega_r^2 - 1)$. The coefficient of $O(\beta^{\frac{1}{3}})$ in the above expression was verified through numerical results for the special case $\Omega = 1$ ($\omega_r = \infty$). Next, calculations were made for $N = 8$ with the bubbles now placed on a lattice of half the size of the cube. Since the overall geometry is the same as for $N = 1$, the results for the two should be the same, and this was found to be the case. It may be noted that the bubble-interaction effects only cause a shift in the resonance frequency of the bubbly liquid from the natural frequency of the bubbles when they are arranged in a periodic array. Thus, the effective speed-based attenuation applies only to random dispersions.

4.2. *Results or* $\omega_r = 1$

Figure 3 shows the real and imaginary parts of z as a function of the highest order N_s of singularities retained in solving the multi-bubble interaction problem with $\beta = 0.01$ and $\omega_r = 1$, i.e. for the frequency of sound waves equal to the natural frequency of the bubbles. We see that, at such volume fractions, $N_s = 0$ provides an accurate estimate of z. More importantly, we see that the phase speed and attenuation are finite even in the absence of viscous, thermal, or liquid-compressibility effects. This validates the main assumption made in the theory of Sangani (1991), which rearranged (4) to (9).

Figure 4 shows the real and imaginary parts of z for four different configurations of bubbles. The scatter among different configurations is rather small. This is interesting, since one would have expected large scatter at the resonance frequency. The scatter among the strengths of monopoles of different bubbles, i.e. B_{00}^{α}, was also found to be small. Similarly, the effect of N, the number of bubbles per unit cell, was also found to be small. The imaginary part of z for different configurations with $N = 16$ was about 10% lower than those with $N = 40$ and 60. The results for the latter two were

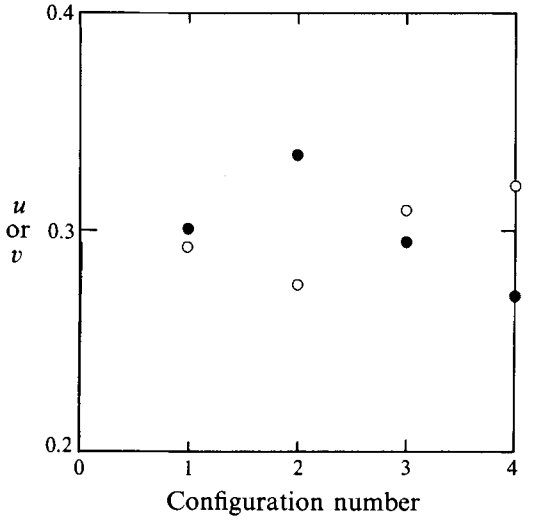

FIGURE 4. The real (open circles) and imaginary (filled circles) parts of z for four different configurations with $N = 40$ and $\beta = 0.01$.

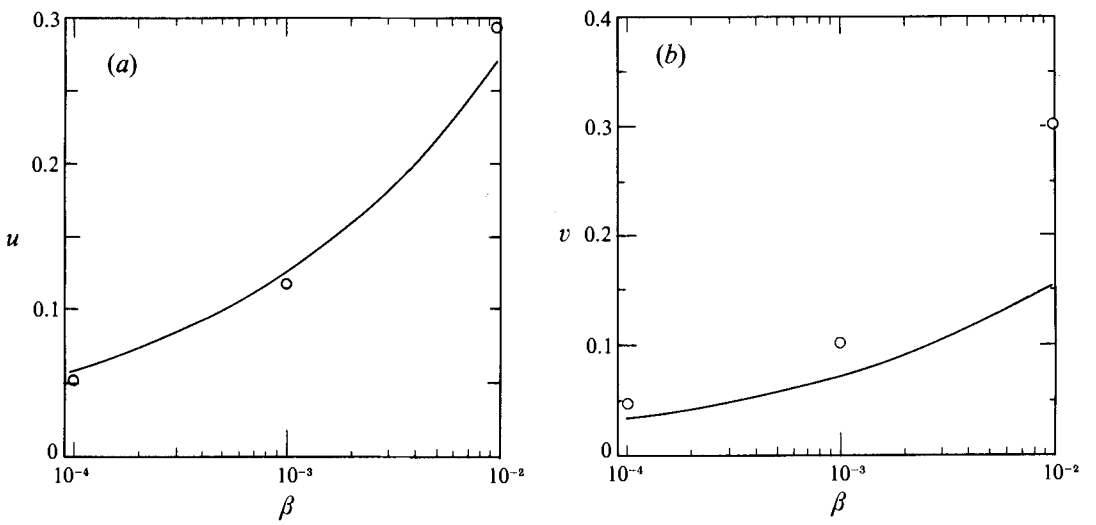

FIGURE 5. A comparison of the numerical simulation results (circles) with the $O(\beta^{\frac{3}{2}})$ theory for $\omega_r = 1$.

essentially the same. The real part of z remained essentially the same as N was increased from 16 to 60. It is interesting to note that z for a periodic array ($N = 1$) is real and equals approximately 0.3, roughly the same as the real part of z for random arrays.

Figure 5 shows the comparison between the simulation results and the modified $O(\beta^{\frac{3}{2}})$ theory (cf. (9)). We see that the two are in agreement for $\beta = 10^{-4}$. The real part of z is in good agreement even at $\beta = 0.01$, while the imaginary part is roughly twice the theoretical value. Thus, the higher-order interactions are significant at $\beta = 0.01$.

It is interesting to note that for most of these configurations we have observed multiple solutions for Γ or, equivalently, z. For example, with $\omega_r = 1$, $\beta = 0.01$, and $N = 40$, the two roots with one configuration of bubbles were $z = 0.275 - 0.335\mathrm{i}$ and $z = -0.395\mathrm{i}$, and with another configuration, they were $z = 0.309 - 0.294\mathrm{i}$ and

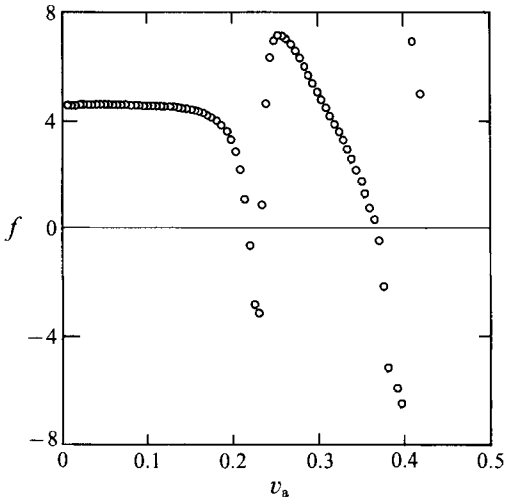

FIGURE 6. The function f (cf. (54)) versus v_a. The zeros of this function represent the solutions for the effective wavenumber by $z = -iv_a$.

$z = -0.345i$. This was observed for other configurations also, both for $N = 16$ and 60, and the magnitude of the roots does not seem to depend on the choice of N. Similarly, the multiple roots were observed for other values of β also. The purely imaginary root corresponds to $z = -3\beta^{\frac{1}{3}}i$, which is the same as that given by $n = 0$ in (10) except for the sign change. (The iterative method restricted the search for z to negative imaginary parts.) We believe that this root is non-physical because it corresponds to using a radially incoming scattered wave in the expression for the conditionally averaged pressure field in the theory of Sangani (1991). Such scattered waves (e^{ikr}/r) do not decay at infinity when the imaginary part of the effective wavenumber k is negative. An inspection of the numerical results showed very large fluctuations ($O(10^3)$ or greater) in the strengths of monopoles (B_{00}^{α}) for these purely imaginary roots. The fluctuations for the other root, on the other hand, were quite small with a typical variance of $O(1)$.

4.3. *Results for* $\omega_r > 1$

We now present results for larger values of ω_r. In particular, it is interesting to examine the behaviour as $\omega_r \to \infty$, k_L being zero. In this limit, the boundary condition for the spherically symmetric part of the pressure around each bubble is the same as that encountered in the well-known problem of determining the effective reaction rate in a diffusion-controlled medium consisting of spherical sinks randomly dispersed in a medium. The analysis of Mattern & Felderhof (1987) for small volume fraction of sinks applies directly here and yields

$$-z^2 = v^2 = 3\beta[1 + (3\beta)^{\frac{1}{2}} + O(\beta \log \beta)] \quad (\omega_r \to \infty, k_L = 0). \tag{53}$$

Note that z is purely imaginary in this limit. The above expression is the same as that given by (5) with $t_0 = -1$. The results of our numerical solution verify the above asymptote, but we observe multiple solutions in this case also, as shown in figure 6. In this figure, we have plotted the quantity (cf. (44))

$$f(z_a) = t_{00} - F_0^1 - \sum_{r,s,\gamma} [B_{rs}^{\gamma} \mathscr{D}_{rs} + \tilde{B}_{rs}^{\gamma} \tilde{\mathscr{D}}_{rs}] S^*(\mathbf{y}^1 - \mathbf{y}^{\gamma}) e^{i\Gamma_a(y_1^{\gamma} - y_1^1)} \tag{54}$$

versus $v_a = -iz_a$, z_a being the assumed value of z. In the iterative method, we take

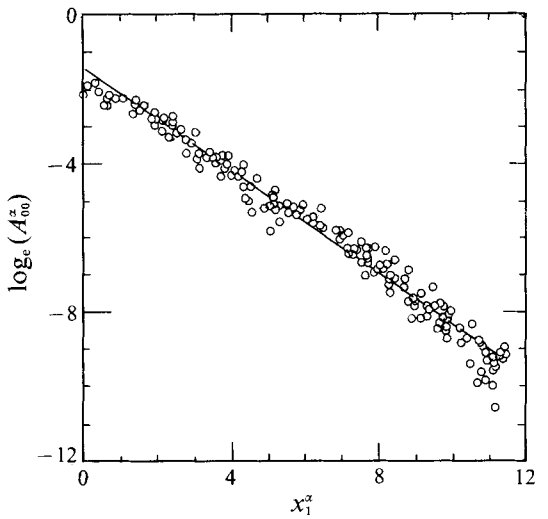

FIGURE 7. Determination of the attenuation by the direct method. The slope of the line $\log_e A^{\alpha}_{00}$ versus v^{α}_1 directly yields the imaginary part of z, and hence the attenuation, at large frequencies for which the real part of z vanishes. $\beta = 0.01$, $k_L = 0$, $\omega_r = 7$, and $N = 200$.

$B^1_{00} = 1$ and after solving for all the other B^{ν}_{rs} for assumed value of z, we determine $f(z_a)$. When z_a is purely imaginary, $f(z_a)$ is real, and therefore z is determined from the zeros of $f(z_a)$. As seen in figure 6, f goes through three zeros and one pole as v_a is varied from zero to 0.41. The first zero is close to that predicted from (53). We may add here that while purely imaginary roots at $\omega_r = 1$ are non-physical, they correspond to an exponential decay of sound intensity for larger ω_r, and thus they are physically permissible. Different roots in this case may be regarded as different eigenvalues, and since the smallest eigenvalue dictates the asymptotic behaviour at large distances, we shall present results for the smallest eigenvalue (first zero) only.

The above results were obtained by the iterative search method. Figure 7 shows the strengths of monopoles (A^{α}_{00}) as a function of x^{α}_1 obtained using the direct method. Thus, these results correspond to the case of wave propagation through a finite region of bubbly liquid. The solid line represents the best linear fit, and the slope of this line gives v for the bulk of bubbly liquid. The result obtained in this manner was found to be in good agreement with the smallest eigenvalue determined by the iterative method.

Figure 8 shows v as a function of frequency for $\beta = 0.01$. The results were obtained using the iterative method and by averaging over three to four configurations. We see that the computed results are in very good agreement with the $O(\beta^{\frac{3}{2}})$ theory of Sangani for $\omega_r > 2$. The significant differences between the theory and simulations occur only in the vicinity of $\omega_r = 1$. The real part of z varies from its value for $\omega_r = 1$ shown in figure 3 to zero for $\omega_r \approx 1.4$, in agreement with the rough estimate given in §2. Beyond this value, z is purely imaginary, and can be estimated using the direct method also.

4.4. *Comparison with experiments*

We now compare the theory and simulations with experimental data on sound attenuation. A number of investigators (Carstensen & Foldy 1947; Fox, Curly & Larson 1955; Silberman 1957; Kol'tsova *et al.* 1979; Ruggles, Scarton & Lahey 1986) have reported data on attenuation of sound waves. Ruggles *et al.* presented results up to $\beta = 0.2$, but they limited their measurements to low frequencies. Other investigators

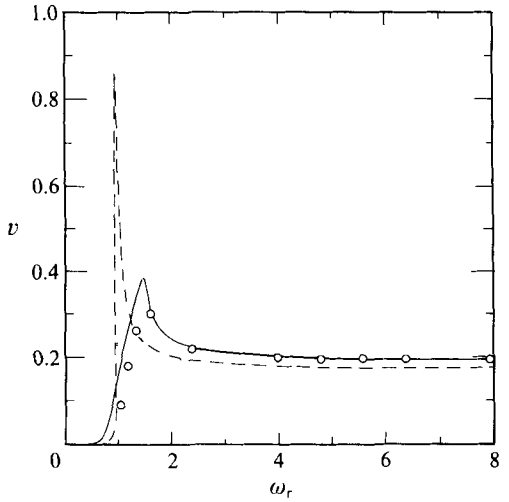

FIGURE 8. A comparison of the numerical simulation results (circles) with the $O(\beta)$ and $O(\beta^{\frac{3}{2}})$ theories denoted, respectively, by the dashed and solid lines. $k_L = b^* = 0$ and $\beta = 0.01$.

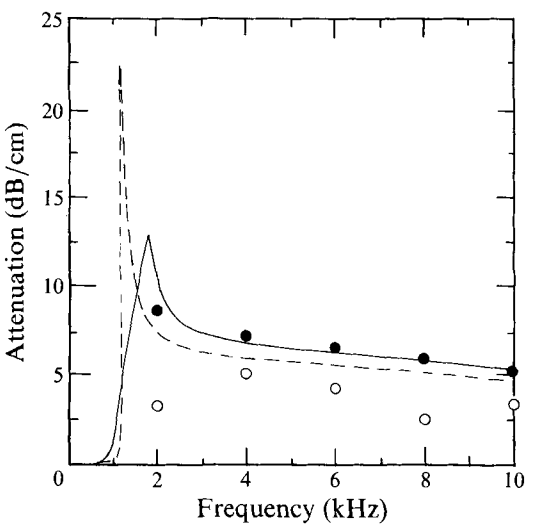

FIGURE 9. A comparison of analytical results with experimental data due to Silberman (1957). The simulation results are denoted by filled circles, the $O(\beta^{\frac{3}{2}})$ theory by the solid line, the $O(\beta)$ theory by the dashed line, and the experimental data by open circles. The radius of the bubbles is 2.6 mm and $\beta = 0.01$.

examined bubbly liquids at low β, and among these, the data by Silberman (1957) are regarded as the best as far as the uniformity of the bubbles' size is concerned. It is for this reason that Sangani (1991) compared his theory only with the data by Silberman. The highest value of β in these experiments was 0.01, and the radius of the bubbles was about 2.6 mm. This corresponds to a natural frequency of 1.4 kHz. The non-adiabatic thermal effects are important for these experimental conditions, and since we wish to investigate the possible effects due to finite compressibility of liquid at higher frequencies, we account for both of these effects in our simulations. The results are shown in figure 9 where the open circles represent the data by Silberman and the filled circles the results of numerical simulations after averaging over four different

configurations with $N = 100$. We see that, while the simulation results agree very well with the $O(\beta^{\frac{3}{2}})$ theory, there is a considerable discrepancy between the simulations and experimental results. This discrepancy at higher frequency occurs in the other data presented by Silberman also. As mentioned earlier, Commander & Prosperetti (1989) have compared Foldy's theory with the data by a number of investigators. From that study it can be seen that the attenuation values predicted by Foldy's theory are generally higher than the experimental values at larger frequencies, and since the predictions from the $O(\beta^{\frac{3}{2}})$ theory are even greater than Foldy's theory, the discrepancy would be observed in comparison with other data also.

We have investigated the effect of polydispersity on the attenuation of waves in bubbly liquids. Thus, we took the radius of bubbles to be given by $a^\alpha = 2.6(1+\xi^\alpha)$ mm with ξ^α being a uniform random variable with a prescribed upper bound on its magnitude. At a frequency of 10 kHz, we found the attenuation to increase monotonically by about 15% as we varied the bound on $|\xi^\alpha|$ from 0 to 0.5. The experimental value reported by Silberman, on the other hand, is lower than the simulation results for monodispersed bubbly liquids.

Our calculations have assumed the bubbles to be spherical, but it is well known that the bubbles of radius 2.6 mm rising under gravity are non-spherical. Since the $O(\beta^{\frac{3}{2}})$ correction to Foldy's theory arises from the consideration of the conditional-averaged pressure field at long distances from the bubble where the shape is not important, we believe that the departure from sphericity is not responsible for the discrepancy between experiments and theory.

Based on Foldy's theory, Silberman assumed the phase speed to be infinite in interpreting his data for $\omega_r > 1$, and this should result in some error in the 1.4–2.0 kHz frequency range, where we have found the phase speed to be finite. This, however, does not explain the discrepancy at higher frequencies. (Note that the numerical and experimental results are shown only for higher frequencies where this effect becomes unimportant.) Finally, we note that Silberman used a different procedure for measuring attenuation at higher frequencies, and it is possible that those measurements may not be accurate.

5. Conclusions

We have devised a method for solving the multiple scattering problem in non-dilute dispersions for which the effective wavelength is of the same order of magnitude as the size of the bubbles. The attenuation and phase speeds are shown to be finite at $\omega_r = 1$ even in the absence of damping due to viscous, thermal or finite liquid compressibility effects. The pairwise interaction theory of Sangani (1991) found a number of resonances among pairs of bubbles (in pure liquid) to cause divergence in the $O(\beta^2)$ correction to Foldy's theory. Numerical results obtained in the present study indicate that such resonance effects are likely to be unimportant in practice.

Sangani (1991) has suggested that a poor agreement between theory and experimentation at higher frequencies may be caused by neglect of the finite compressibility of the liquid or the multi-bubble interactions effects, in particular, due to the out-of-phase mode resonance between pairs of bubbles which occur at higher frequencies. These, and the effect of polydispersity, are examined in the present work, and it is found that none of these can be responsible for the discrepancy.

From the standpoint of comparing predictions of theory with experiments, the range of frequency and β values that are perhaps most interesting are $5 \leqslant \omega_r \leqslant 15$ and $0.01 \leqslant \beta \leqslant 0.05$ as the higher-order theory is substantially different from Foldy's

theory in this range, and attenuation values are not too large to cause uncertainty in their measurements. Unfortunately, adequate experimental data in this range do not exist to conclude whether the theory as it stands needs further improvement.

This work was supported by the Department of Energy and the National Science Foundation under Grants DE-FG02-90ER 14136 and CBT-8800451. The authors are grateful to Dr A. Lezzi for help in providing the proof presented in Appendix C and to Professor A. Prosperetti for valuable suggestions.

Appendix A. Evaluation of H

The fundamental singular solution of the Helmholtz equation with singularities on the lattice in the plane $x_1 = 0$ (cf. (22)) can be shown to be given by

$$H = \frac{1}{\pi\tau}\int_{-\infty}^{\infty} \mathrm{d}s \sum_{q\neq 0} \frac{1}{s^2+q^2-\lambda^2} \mathrm{e}^{-2\pi \mathrm{i}(q\cdot R + s x_1)}, \quad \lambda = k_L/2\pi, \tag{A 1}$$

where q is the reciprocal lattice vector, $R = x_2 e_2 + x_3 e_3$, and τ is the area of the unit cell. For a square lattice of spacing h, $\tau = h^2$ and $q = h^{-1}(m e_2 + n e_3)$, m and n being integers. The summation in q in the above expression is to be carried out for all combinations of m and n except $m = n = 0$. Finally, e_2 and e_3 are the unit vectors along the x_2- and x_3-axes, respectively.

The above expression for H diverges when $k_L h > 2\pi$, for which denominator vanishes for some values of q and s. This, of course, corresponds to the resonance behaviour of the lattice, and, as is well known, the damping due to viscous or other effects will be important close to this resonance. For the range of frequencies in which we are interested in the present study, $k_L R$ is small. For example, with bubbles of radii 0.26 cm, and a frequency of 10 kHz ($\omega = 2\pi \times 10^4\ s^{-1}$), $k_L R$ is approximately 0.1. Thus, $k_L h$ equals 2π when h/R or $(4\pi N/3\beta)^{\frac{1}{3}}$ becomes approximately equal to 60. For a given β, the resonance behaviour of the planar lattice will therefore become important if N is sufficiently large and render the model of artificially imposed periodicity in the plane transverse to the propagation invalid for describing the behaviour of truly random bubbly liquid. For low values of β ($\leqslant 0.01$), this corresponds to a rather large N ($\geqslant 500$). Since most of the results presented here were obtained with $N \leqslant 200$, this limitation due to imposed periodicity is not significant.

For completeness, we shall give expressions for evaluating H for all values of $k_L h$. To obtain finite H, we shall assume that a small viscous damping is present. This amounts to replacing λ^2 in (A 1) by $\lambda^2 - \mathrm{i}\epsilon$, with $\epsilon = \mu k_L^4/3\pi^2\rho_L\omega$. For the air–water system at 10 kHz, ϵ is $O(10^{-9})$.

On integrating with respect to s, (A 1) reduces to

$$H = \sum_{q\neq 0} \frac{1}{\gamma_q \tau} \mathrm{e}^{-2\pi\gamma_q |x_1|} \cos(2\pi q\cdot R), \tag{A 2}$$

where γ_q is a complex quantity defined by

$$\left.\begin{aligned} \gamma_q &= (q^2-\lambda^2+\tfrac{1}{2}\epsilon)^{\frac{1}{2}} + \mathrm{i}\frac{\frac{1}{2}\epsilon}{(q^2-\lambda^2+\frac{1}{2}\epsilon)^{\frac{1}{2}}}, \quad q > \lambda, \\ \gamma_q &= \frac{\frac{1}{2}\epsilon}{(\lambda^2-q^2+\frac{1}{2}\epsilon)^{\frac{1}{2}}} + \mathrm{i}(\lambda^2-q^2+\tfrac{1}{2}\epsilon)^{\frac{1}{2}}, \quad q \leqslant \lambda. \end{aligned}\right\} \tag{A 3}$$

Note that some of the γ_q become purely imaginary in the limit $\epsilon \to 0$ whenever $k_L h > 2\pi$.

Equation (A 2) is useful when $|x_1|$ is not small, for which it converges rapidly. For small $|x_1|$ we use the Ewald's technique and write

$$H = \mathrm{I} + \mathrm{II} + \mathrm{III}, \tag{A 4}$$

with

$$\mathrm{I} = \frac{2}{\tau} \sum_{q \neq 0} \int_0^\infty \frac{\mathrm{d}s \cos 2\pi s x_1}{\pi(s^2 + q^2 - \lambda^2 + \mathrm{i}\epsilon)} \mathrm{e}^{-\pi\alpha(s^2+q^2-\lambda^2+\mathrm{i}\epsilon)} \mathrm{e}^{-2\pi \mathrm{i} \boldsymbol{q}\cdot\boldsymbol{R}}, \tag{A 5}$$

$$\mathrm{II} = \frac{2}{\tau} \sum_{q} \int_0^\infty \mathrm{d}s \cos 2\pi s x_1 \int_0^\alpha \mathrm{d}y \, \mathrm{e}^{-\pi y(s^2+q^2-\lambda^2+\mathrm{i}\epsilon)} \mathrm{e}^{2\pi i \boldsymbol{q}\cdot\boldsymbol{R}}, \tag{A 6}$$

$$\mathrm{III} = -\frac{2}{\tau} \int_0^\infty \mathrm{d}s \cos 2\pi s x_1 \int_0^\alpha \mathrm{d}y \, \mathrm{e}^{-\pi y(s^2-\lambda^2+\mathrm{i}\epsilon)}, \tag{A 7}$$

where α is a constant to be chosen such that the sums in I and II converge rapidly. The final result for H is, of course, independent of the choice of α.

Performing the integration over s in (A 5) yields

$$\mathrm{I} = \sum_{q \neq 0} \frac{1}{2\tau\gamma_q} \left[2\cosh(2\pi x_1 \gamma_q) - \mathrm{e}^{-2\pi x_1 \gamma_q} \operatorname{erf}\left(\gamma_q (\pi\alpha)^{\frac{1}{2}} - \frac{\pi x_1}{(\pi\alpha)^{\frac{1}{2}}} \right) - \mathrm{e}^{2\pi x_1 \gamma_q} \operatorname{erf}\left(\gamma_q (\pi\alpha)^{\frac{1}{2}} + \frac{\pi x_1}{(\pi\alpha)^{\frac{1}{2}}} \right) \right] \cos(2\pi \boldsymbol{q}\cdot\boldsymbol{R}), \tag{A 8}$$

where erf is the error function, and γ_q is defined by (A 3).

To evaluate II, we first apply the theta transformation formula for converting the sum over two-dimensional reciprocal vectors $\boldsymbol{q}$ to that over the lattice vectors $\boldsymbol{R}_L$

$$\frac{1}{\tau} \sum_{q} \mathrm{e}^{-\pi y q^2 - 2\pi i \boldsymbol{q}\cdot\boldsymbol{R}} = \frac{1}{y} \sum_{R_L} \mathrm{e}^{-\pi |\boldsymbol{R} - \boldsymbol{R}_L|^2 / y} \tag{A 9}$$

to yield

$$\mathrm{II} = 2 \sum_{R_L} \int_0^\infty \mathrm{d}s \cos(2\pi s x_1) \int_0^\alpha \frac{\mathrm{d}y}{y} \mathrm{e}^{-\pi y(s^2-\lambda^2)} \mathrm{e}^{-\pi |\boldsymbol{R} - \boldsymbol{R}_L|^2 / y}, \tag{A 10}$$

where we have set $\epsilon = 0$ since II is regular in the limit $\epsilon \to 0$. Performing the integrations over s and y, we obtain

$$\mathrm{II} = \sum_{R_L} \frac{\cos k_L r_L}{r_L} - \frac{1}{2r_L} \left\{ \mathrm{e}^{-2\pi \mathrm{i} r_L \lambda} \operatorname{erf}\left(\left(\frac{\pi}{\alpha}\right)^{\frac{1}{2}} r_L - \mathrm{i}(\pi\alpha)^{\frac{1}{2}} \lambda \right) + \mathrm{e}^{2\pi \mathrm{i} r_L \lambda} \operatorname{erf}\left(\left(\frac{\pi}{\alpha}\right)^{\frac{1}{2}} r_L + \mathrm{i}(\pi\alpha)^{\frac{1}{2}} \lambda \right) \right\}, \tag{A 11}$$

where $r_L = |\boldsymbol{R} + x_1 \boldsymbol{e}_1 - \boldsymbol{R}_L|$.

Finally, (A 7) for III simplifies to

$$\mathrm{III} = \frac{\sin(k_L |x_1|)}{\lambda\tau} + \frac{\mathrm{i}}{2\tau\lambda} \left[\mathrm{e}^{2\pi \mathrm{i} \lambda x_1} \operatorname{erf}\left(\left(\frac{\pi}{\alpha}\right)^{\frac{1}{2}} x_1 + \mathrm{i}\lambda(\pi\alpha)^{\frac{1}{2}} \right) + \mathrm{e}^{-2\pi \mathrm{i} \lambda x_1} \operatorname{erf}\left(-\left(\frac{\pi}{\alpha}\right)^{\frac{1}{2}} x_1 + \mathrm{i}\lambda(\pi\alpha)^{\frac{1}{2}} \right) \right], \tag{A 12}$$

where, once again, we have set $\epsilon = 0$ as III is also regular in the limit $\epsilon \to 0$.

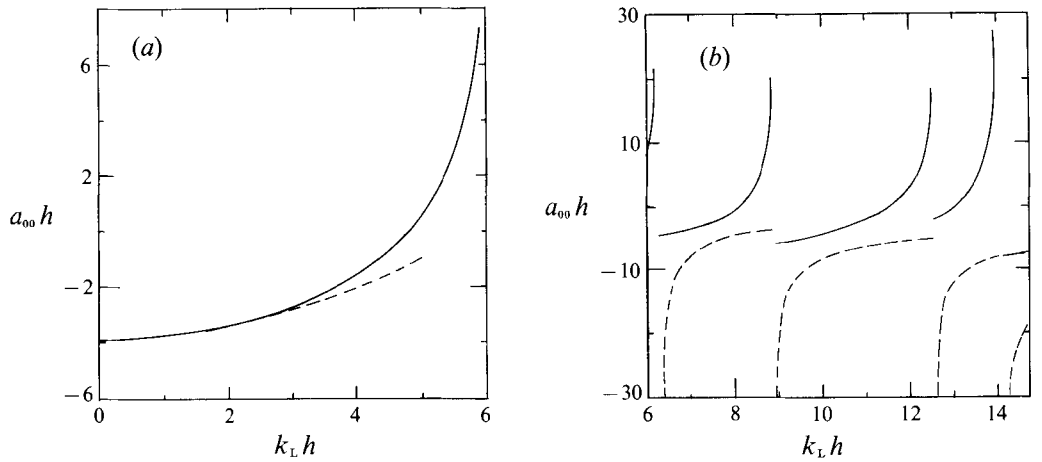

FIGURE 10. a_{00} as a function of $k_L h$. (*a*) For $k_L h < 6$, a_{00} is essentially real and the computed values are shown by the solid line. The dashed curve is the asymptotic relation (A 14). (*b*) For higher values of $k_L h$, a_{00} is complex due to lattice resonance effects, and real and imaginary parts are denoted, respectively, by solid and dashed lines.

It is interesting to note the behaviour of H near its singularities. II and III are singular, respectively, at the lattice points and at $x_1 = 0$. These correspond to the singularities in the differential equation for H (cf. (22)). In addition, we have singularities in I for certain values of $k_L h$ due to the resonance of the doubly periodic lattice. The behaviour very close to this last set of singularities depends explicitly on the magnitude of ϵ. We see that the singularity in II near each lattice point corresponds to a standing radial wave and in III to a standing planar wave. This standing-wave behaviour arises because of the imposed periodicity.

Near $r = 0$, H can be expanded as

$$H = \frac{\cos(k_L r)}{r} + \frac{\sin(k_L|x_1|)}{\lambda\tau} + \sum_{n=0}^{\infty}\sum_{m=0}^{n} h^{-1} a_{nm} j_n(k_L r) P_n^m(\cos\theta)\cos m\varphi, \quad \text{(A 13)}$$

where a_{nm} is a function of $k_L h$ and the geometry of the lattice. In particular, a_{00} can be determined by first removing the singularities from II and III and then substituting $x = 0$. The results of the computations are shown in figure 10. As $k_L h \to 0$, we find

$$a_{00} \to -3.900 - 0.1144(k_L h)^2. \quad \text{(A 14)}$$

The constants in (A 14) agree with those appearing in the fundamental singular solutions of the Stokes and Laplace equations derived earlier by Sangani & Behl (1989). More specifically, it is easy to show that H can be expanded for small $k_L h$ as

$$H = \Psi_1 - k_L^2 \Psi_2 + k_L^4 \Psi_3 + \ldots, \quad \text{(A 15)}$$

with Ψ_m satisfying

$$\nabla^2 \Psi_1(\boldsymbol{x}) = \frac{4\pi}{h^2}\delta(x_1) - 4\pi \sum_{\boldsymbol{R}_L} \delta(\boldsymbol{x} - \boldsymbol{R}_L), \quad \nabla^2 \Psi_m = \Psi_{m-1}, \quad m \geqslant 2. \quad \text{(A 16)}$$

As seen in figure 10, the behaviour of a_{00} is considerably influenced by the resonance of the lattice for $k_L h > 2\pi$, and, therefore, the imposed periodicity will strongly affect the behaviour of the bubbly liquid when h is very large. One would have expected that $H \to e^{-ik_L x}/r$ as $h \to \infty$ since each lattice point would then behave as an isolated scatterer. The results of computations, however, indicate that this is not to be the case.

Appendix B. Equations for determining the fully developed solution

The long-range part $P_n^{\alpha l}$ in (40) and (41) can be expressed as

$$P_n^{\alpha l} = (-\mathrm{i}k)^n \mathrm{e}^{-\mathrm{i}kx_1^{\alpha l}} + c \sum_{r,\gamma,j} \{(-\mathrm{i}k)^{r+n} a_{\alpha l}^{\gamma j} \mathrm{e}^{-\mathrm{i}k(x_1^{\alpha l}-x_1^{\gamma j})} + (\mathrm{i}k)^{r+n} b_{\alpha l}^{\gamma j} \mathrm{e}^{\mathrm{i}k(x_1^{\alpha l}-x_1^{\gamma j})}\} A_{r0}^{\gamma j}, \quad \text{(B 1)}$$

where $a_{\alpha l}^{\gamma j} = g(x_1^{\alpha l} - x_1^{\gamma j})$, $b_{\alpha l}^{\gamma j} = 1 - a_{\alpha l}^{\gamma j}$, and, for brevity, we have taken $k = k_{\mathrm{L}}$. $g(x)$ is the Heavyside step function whose value is unity for $x > 0$, zero for $x < 0$, and one-half for $x = 0$. Now substituting (43) into (B 1), using $x_1^{\alpha l} = y_1^{\alpha} + (l-1)h$, and carrying out summation over j using identities

$$\sum_{j=1}^{l-1} \mathrm{e}^{s(j-1)} = \frac{1-\mathrm{e}^{s(l-1)}}{1-\mathrm{e}^{s}}, \quad \sum_{j=1}^{N_{\mathrm{c}}} \mathrm{e}^{s(j-1)} = \frac{\mathrm{e}^{sN_{\mathrm{c}}} - \mathrm{e}^{s(l-1)}}{\mathrm{e}^{s}-1}, \quad \text{(B 2)}$$

we obtain

$$P_n^{\alpha l} = (-\mathrm{i}k)^n \mathrm{e}^{-\mathrm{i}kx_1^{\alpha l}} + c \sum_{r,\gamma} \Bigg[B_{r0}^{\gamma} \Bigg\{ \left(\frac{1-\mathrm{e}^{\mathrm{i}(k+\Gamma)h(l-1)}}{1-\mathrm{e}^{\mathrm{i}(k+\Gamma)h}} + \lambda_{\alpha\gamma} \mathrm{e}^{\mathrm{i}(k+\Gamma)h(l-1)} \right) \times (-\mathrm{i}k)^{n+r} \mathrm{e}^{\mathrm{i}(k+\Gamma)y_1^{\gamma}} \mathrm{e}^{-\mathrm{i}kx_1^{\alpha l}} + \left(\frac{\mathrm{e}^{\mathrm{i}(\Gamma-k)hN_{\mathrm{c}}} - \mathrm{e}^{\mathrm{i}(\Gamma-k)h(l-1)}}{\mathrm{e}^{\mathrm{i}(\Gamma-k)h}-1} - \lambda_{\alpha\gamma} \mathrm{e}^{\mathrm{i}(\Gamma-k)h(l-1)} \right) \times (\mathrm{i}k)^{n+r} \mathrm{e}^{\mathrm{i}(\Gamma-k)y_1^{\gamma}} \mathrm{e}^{\mathrm{i}kx_1^{\alpha l}} \Bigg\} + \text{p.t.} \Bigg], \quad \text{(B 3)}$$

where $\lambda_{\alpha r} = g(y_1^{\alpha} - y_1^{\gamma})$, and p.t. stands for the primed terms obtained by replacing B_{r0} and Γ with B'_{r0} and Γ', respectively.

The short-range part in (40), upon substituting for $A_{nm}^{\alpha l}$ from (43), is given by

$$\sum_{r,s,\gamma} \sum_{j=1}^{N_{\mathrm{c}}} (B_{rs}^{\gamma} \mathscr{D}_{rs} + \tilde{B}_{rs}^{\gamma} \tilde{\mathscr{D}}_{rs}) \mathscr{D}_{nm} H^*(\boldsymbol{x}^{\alpha l} - \boldsymbol{x}^{\gamma j}) + \text{p.t.} \quad \text{(B 4)}$$

Since H decays exponentially, the summation over j can be extended to all integers to give the following approximation for the short-range part:

$$\mathrm{e}^{\mathrm{i}\Gamma x_1^{\alpha l}} \sum_{r,s,\gamma} \mathrm{e}^{\mathrm{i}\Gamma(y_1^{\gamma} - y_1^{\alpha})} [B_{rs}^{\gamma} \mathscr{D}_{rs} + \tilde{B}_{rs} \tilde{\mathscr{D}}_{rs}] \mathscr{D}_{nm} \sum_{m=-\infty}^{\infty} H^*(\boldsymbol{y}^{\alpha} - \boldsymbol{y}^{\gamma} + mh\boldsymbol{e}_1) \mathrm{e}^{-\mathrm{i}mh\Gamma} + \text{p.t.}, \quad \text{(B 5)}$$

where $m = l - j$ and the derivatives of H^* are to be evaluated with respect to $\boldsymbol{y}^{\alpha} - \boldsymbol{y}^{\gamma}$. The approximation is valid when the bubble αl is in the bulk of the bubbly region.

In order that (40) permits a solution in the form given by (43), the coefficients of $e^{\mathrm{i}k_{\mathrm{L}}x_1^{\alpha l}}$ and $\mathrm{e}^{-\mathrm{i}k_{\mathrm{L}}x_1^{\alpha l}}$ in the long-range part $P_n^{\alpha l}$ must vanish for all α, l, and n. It can be easily verified that these conditions are satisfied provided that

$$0 = 1 + c \sum_{r,\gamma} \left[(-\mathrm{i}k_{\mathrm{L}})^r B_{r0}^{\gamma} \frac{\mathrm{e}^{\mathrm{i}(\Gamma+k_{\mathrm{L}})y_1^{\gamma}}}{1-\mathrm{e}^{\mathrm{i}(\Gamma-k_{\mathrm{L}})h}} + \text{p.t.} \right]$$

$$= c \sum_{r,\gamma} \left[(\mathrm{i}k_{\mathrm{L}})^r B_{r0}^{\gamma} \mathrm{e}^{\mathrm{i}(\Gamma-k_{\mathrm{L}})y_1^{\gamma}} \frac{\mathrm{e}^{\mathrm{i}(\Gamma-k_{\mathrm{L}})hN_{\mathrm{c}}}}{\mathrm{e}^{\mathrm{i}(\Gamma-k_{\mathrm{L}})h}-1} + \text{p.t.} \right]. \quad \text{(B 6)}$$

The coefficients of the terms multiplying $\mathrm{e}^{\mathrm{i}\Gamma x_1^{\alpha l}}$ and $\mathrm{e}^{\mathrm{i}\Gamma' x_1^{\alpha l}}$ in the equations that result upon substituting the expressions for $P_n^{\alpha l}$ and the short-range contributions given in this appendix into (40) and (42) can be set to zero to determine Γ, B_{rs}^{γ}, $\tilde{B}_{rs}^{\gamma}$, and the corresponding quantities with a tilde in terms of any two unknowns, say B_{00}^{1} and $B_{00}^{1\prime}$. Finally, these two unknowns can be determined in principle from the two equations

given by (B 6). Thus, we have the necessary and sufficient conditions for uniquely determining the solution in the bulk. The equations that result by comparing the coefficients of $e^{i\Gamma x_1^{\alpha l}}$ are given by (44)–(46).

Appendix C. Special cases

In this appendix, we show that the results obtained by Foldy (1945) and Rubinstein (1985) can be derived from the equations given in §3. In Foldy's analysis the bubbles act as independent monopole scatterers, the interaction among pairs of bubbles and higher-order multipoles being negligible. Taking therefore $B_{00}^{\alpha} = 1$, and setting all the higher-order multipoles to zero, yields

$$F_0^{\alpha} = \frac{4\pi}{h^2} \sum_{\gamma=1}^{N} \left\{ (y_1^{\alpha} - y_1^{\gamma}) \left(\frac{1}{e^{i\Gamma h} - 1} + \lambda_{\alpha\gamma} \right) - \frac{h e^{i\Gamma h}}{(e^{i\Gamma h} - 1)^2} \right\} e^{i\Gamma(y_1^{\gamma} - y_1^{\alpha})}. \tag{C 1}$$

Now in the limit of $N \to \infty$, we can replace the sum in (C 1) by an integral to yield

$$F_0^{\alpha} = \frac{4\pi N}{h^3} \int_{-h/2}^{h/2} dy \left\{ \frac{y e^{i\Gamma y}}{e^{i\Gamma h} - 1} + g(-y)\, y e^{i\Gamma y} - \frac{h e^{i\Gamma(y+h)}}{(e^{i\Gamma h} - 1)^2} \right\}, \tag{C 2}$$

where $y = y_1^{\gamma} - y_1^{\alpha}$. In approximating the sum by integral, we have made an assumption that the bubbles are uniformly distributed in a cube of size h. On evaluating the integral, substituting for F_0^{α} into (44), and neglecting the short-range interaction part in that equation which accounts for interaction among bubbles, we obtain

$$t_{00} = 4\pi N / h^3 \Gamma^2. \tag{C 3}$$

Now substituting for t_{00} from (39), and using $\beta = 4\pi N R^3 / 3h^3$, we see that (C 3) reduces to the Foldy's result (cf. (1)) with $z_L = 0$.

Rubinstein (1985) examined dilute periodic arrays. His results can be obtained by taking $N = 1$ and neglecting higher-order multipoles. He obtained the leading-order correction to the Foldy's approximation by accounting for the interactions among the bubbles. Therefore retaining the short-range part in (44), we now obtain

$$t_{00} = -\frac{4\pi}{h} \frac{e^{i\Gamma h}}{(e^{i\Gamma h} - 1)^2} + S^*(0). \tag{C 4}$$

For the special case of $z_L = 0$, S^* is given by

$$S^*(0) = \sum_{l=-\infty}^{\infty} \Psi_1^*(lhe_1)\, e^{-i\Gamma l h}, \tag{C 5}$$

where Ψ_1^* is the regular part of the doubly periodic singular solution of Laplace equation (cf. (A 16)). Now (C 4) can be recast as

$$\sin^2 \tfrac{1}{2}\Gamma h = \frac{\pi}{h(t_{00} - S^*(0))}, \tag{C 6}$$

and noting that t_{00} is inversely proportional to R, we see that, to leading order, $(\Gamma h)^2$ is $O(R/h)$ or $O(\beta^{\frac{1}{3}})$. This corresponds to Foldy's approximation. To obtain the next correction, it is necessary to expand only the sinusoidal function in (C 6) for small Γh; $S^*(0)$ may be evaluated by taking $\Gamma = 0$. This yields

$$\Gamma^2 = \frac{4\pi}{h^3 [t_{00} - (\pi/(3h) + \sum \Psi_1^*(lhe_1))]}, \tag{C 7}$$

where the summation in l is over all integers. Rubinstein (1985) obtained his expression in terms of the periodic singular solution S_1 for a triply periodic lattice. Comparing (C 7) with Rubinstein's results, we see that the two agree provided that

$$D^*(0) \equiv S_1^*(0) - \sum \Psi_1^*(lhe_1) = \frac{\pi}{3h}. \tag{C 8}$$

To evaluate $D^*(0)$, we start with the differential equation

$$\frac{\mathrm{d}^2 D}{\mathrm{d}x_1^2} = \frac{4\pi}{h^3}\left[1 - h \sum_{l=-\infty}^{l=\infty} \delta(x_1 - lh)\right] \tag{C 9}$$

obtained by subtracting the governing differential equations for S_1 and Ψ_1 (Hasimoto 1959; Sangani & Behl 1989). Upon solving the above differential equation and evaluating D at $x_1 = 0$, we verify (C 8), and thus the present analysis is in agreement with the analysis of Rubinstein (1985) for dilute periodic arrays.

REFERENCES

Abramowitz, M. & Stegun, I. A. 1972 *Handbook of Mathematical Functions with Formulas, Graphs, and Mathematical Tables.* National Bureau of Standards.

Bensoussan, A., Lions, J.-L. & Papanicolaou, G. C. 1978 *Studies in Mathematics and Its Applications*, vol. 5. North-Holland.

Caflisch, R. E., Miksis, M. J., Papanicolaou, G. C. & Ting, L. 1985*a* Effective equation for wave propagation in bubbly liquids. *J. Fluid Mech.* **153**, 259.

Caflisch, R. E., Miksis, M. J., Papanicolaou, G. C. & Ting, L. 1985*b* Wave propagation in bubbly liquids at finite volume fraction. *J. Fluid Mech.* **160**, 1.

Carstensen, E. L. & Foldy, L. L. 1947 Propagation of sound through a liquid containing bubbles. *J. Acoust. Soc. Am.* **19**, 481.

Commander, K. W. & Prosperetti, A. 1989 Linear pressure waves in bubbly liquids: Comparison between theory and experiments. *J. Acoust. Soc. Am.* **85**, 732.

Foldy, L. L. 1945 The multiple scattering of waves. *Phys. Rev.* **67**, 107.

Fox, F. E., Curley, S. R. & Larson, G. S. 1955 Phase velocity and absorption measurements in water containing air bubbles. *J. Acoust. Soc. Am.* **19**, 481.

Hasimoto, H. 1959 On the periodic fundamental singular solutions of the Stokes equations and their application to viscous flow past a cubic array of spheres. *J. Fluid Mech.* **5**, 317.

Hobson, E. W. 1931 *The Theory of Spherical and Ellipsoidal Harmonics.* Cambridge University Press.

Keller, J. B. 1977 Effective behavior of heterogeneous media. *Statistical Mechanics and Statistic Methods in Theory and Application* (ed. U. Landman), p. 631. Plenum.

Kol'tsova, I. S., Krynskii, L. O., Mikhalov, I. G. & Pokrovskaya, I. E. 1979 Attenuation of ultrasonic sound waves in low-viscosity liquids containing gas bubbles. *Akust. Zh.* **25**, 725. (English transl: *Sov. Phys. Acoust.* **25**, 409.)

Mattern, K. & Felderhof, B. U. 1987 Self-consistent cluster expansion for wave propagation and diffusion-controlled reactions in a random medium. *Physica* A **143**, 21.

Miksis, M. J. & Ting, L. 1987*a* Viscous effects on wave propagation in a bubbly liquid. *Phys. Fluids* **30**, 1683.

Miksis, M. J. & Ting, L. 1987*b* Wave propagation in a multiphase media with viscous and thermal effects. *ANS Proc. Natl Heat Transfer Conf.*, p. 145.

Prosperetti, A. 1984 Bubble phenomena in sound fields: part one. *Ultrasonics* **22**, 69.

Rubinstein, J. 1985 Bubble interaction effects on waves in bubbly liquids. *J. Acoust. Soc. Am.* **77**, 2061.

Ruggles, A. E., Scarton, H. A. & Lahey, R. T. 1986 An investigation of the propagation of pressure perturbations in bubbly air/water flows. In *First Intl Multiphase Fluids Transients Symp.* (ed. H. H. Safwat, J. Braun & U. S. Rohatgi). ASME.

SANCHEZ-PALENCIA, E. 1980 *Non-Homogeneous Media and Vibration Theory*. Lecture Notes in Physics, vol. 127. Springer.

SANGANI, A. S. 1991 A pairwise interaction theory for determining the linear acoustic properties of dilute bubbly liquids. *J. Fluid Mech.* **232**, 221.

SANGANI, A. S. & BEHL, S. 1989 The planar periodic singular solutions of Stokes and Laplace equations and their application to transport processes near porous surfaces. *Phys. Fluids* A **1**, 21.

SANGANI, A. S., ZHANG, D. Z. & PROSPERETTI, A. 1991 The added mass, Basset, and viscous drag coefficients in nondilute bubbly liquids undergoing small-amplitude oscillatory motion. *Phys. Fluids* A **3**, 2955.

SILBERMAN, E. 1957 Sound velocity and attenuation in bubbly mixtures measured in standing wave tubes. *J. Acoust. Soc. Am.* **29**, 925.

TWERSKY, V. 1962 On scattering of waves by random distributions. I. Free-space scatterer formalism. *J. Math. Phys.* **3**, 700.

WIJNGAARDEN, L. VAN 1972 One-dimensional flow of liquids containing small bubbles. *Ann. Rev. Fluid Mech.* **4**, 369.